Quantification of shoulder and elbow passive moments in the sagittal plane as a function of adjacent angle fixations

Timotej Kodek and Marko Munih
Faculty of electrical engineering, University of Ljubljana, Slovenia Laboratory for robotics, Tr žaška 25, 1000 Ljubljana, Slovenia
Tel.: +386 1 4768465; Fax: +386 1 4768239; E-mail: {timotej.kodek,marko.munih}@robo.fe.uni-lj.si

Abstract. The goal of this study was an assessment of the shoulder and elbow joint passive moments in the sagittal plane for six healthy individuals. Either the shoulder or elbow joints were moved at a constant speed, very slowly throughout a large portion of their range by means of an industrial robot. During the whole process the arm was held fully passively, while the end point force data and the shoulder, elbow and wrist angle data were collected. The presented method unequivocally reveals a large passive moment adjacent angle dependency in the central angular range, where most everyday actions are performed. It is expected to prove useful in the future work when examining subjects with neuromuscular disorders. Their passive moments may show a fully different pattern than the ones obtained in this study.

Keywords: Elbow passive moments, shoulder passive moments, dynamic model, upper extremity, static movement, sagittal plane, industrial robot

1. Introduction

The passive moments exerted in the human muskuloskeletal system are an internal property of every joint in the upper and lower extremities. They arise mostly from the presence and deformations of structures such as tendons, ligaments, skin, joint capsules, inactive muscles and bones [12,13] composing a particular joint. They could be expressed in terms of elastic and dissipative contributions [12]. Several authors in the past concentrated only on the elastic effects [13,19]. There have been a large number of studies dealing with these properties, out of which the majority were concentrated on lower extremities [16,19,25]. In addition to examining torque-angle properties for one joint, many authors have attempted to construct a model expressing the passive moments as a function of the two adjacent joint angles. Most [12,19] have used a technique proposed by Audu and Davy [2] where this function was taken to be a double exponential curve, indicating a significant torque increase at extreme angles. On the other hand, Hatze [13] proposed a model, consisting of a sum of several individual tissue exponential contributions relating to an observed joint. This relation was further simplified into a hyperbolic one, requiring an identification of a total of 53 elastic and viscous parameters for each degree of freedom in the human elbow joint (i.e. flexion-extension and pronation-supination). It has to be pointed out that all these studies were made without any voluntary muscle action.

There has also been a number of studies concentrating on the arm dynamics in the presence of a voluntary movement, particularly in the elbow joint. Following a study on torques produced in the elbow

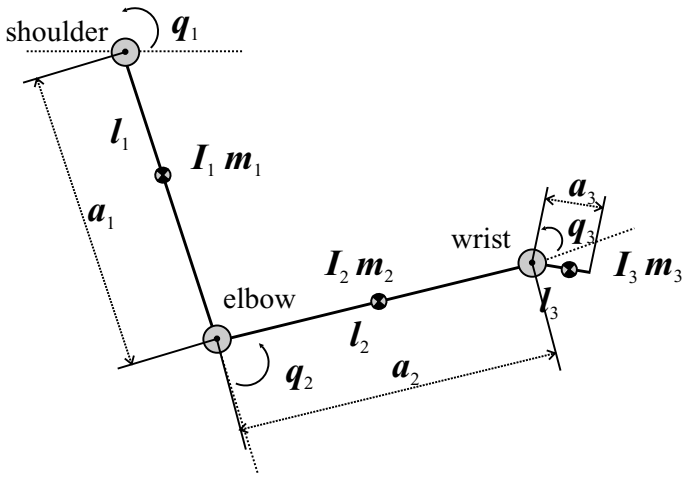

Fig. 1. Geometric definitions for the assumed human arm structure, consisting of three segments.

joint with voluntary movements [3], Bennett and Hollerbach et al. [4] devised an ensemble parametric method for identifying the time-varying compliance of the human elbow joint, using an airjet actuator apparatus. Further studies by Xu and Hollerbach [23,24] on the elbow joint mechanical properties concentrated on estimating elasticity, viscosity and inertial contributions during a voluntary movement, using a similar technique and a two-dimensional device capable of imposing random torque perturbations. In all these studies, the inertia contribution was shown to remain constant despite the varying voluntary muscle action, whereas elasticity and viscosity, both increased and decreased proportionally with the applied muscle force. A number of other studies concentrated on the endpoint stiffness of the human arm mechanism, as a result of all upper limb joint mechanical properties acting in concert [1,17,18].

The studies of Engin et al. concentrated mostly on the shoulder joint. They dealt extensively with kinematics of the human shoulder complex [5–7] and also investigated its passive resistive properties [8, 10,11]. A study of passive resistive properties limited to an area beyond the full elbow extension was also performed [9]. A comprehensive analysis of the kinematic and dynamic behavior of the shoulder mechanism providing a good insight into mechanics of the shoulder mechanism, was presented by Van der Helm [14]. Some parameters acquired in the study of Veeger et al. [22] were also a good lead to our study.

Unlike the work of Xu and Hollerbach [23,24], the study presented here is aimed at separating the effects of passive and active muskuloskeletal contributions to the human arm dynamics. This work firstly concentrates on identifying the passive moments (i.e. elasticity, and dissipative effects) of the elbow and shoulder joints being moved one at a time through a large portion of their flexion-extension range in the sagittal plane. This was achieved by imposing slow (i.e. static) angular movements to a particular joint, while keeping the second joint at a fixed angle. The wrist passive moment was also acquired in the process, but was not thoroughly investigated, because the joint was not displaced. The upper extremity was modelled in terms of an inverse dynamics equation for a three segment planar manipulator [20,21].

The aim of the presented study is providing an alternative upper extremity clinical evaluation method which could be used on patients suffering from neuromuscular disorders usually following a stroke. Passive moment patterns obtained from such subjects are expected to show noticeable differences from the healthy ones.

2. Methods

2.1. Mathematical modeling

In this experimental work the human arm was described as a three degree of freedom kinematic and dynamic structure (Fig. 1). The segment lengths are denoted with a_i, their centers of mass with l_i while q_i indicate the positive angle directions with respect to the zero position (dashed line). Positive angle values are denoted with the arrow. The masses and inertias are presented with the m_i and I_i variables. The centers of gravity were expressed as a distal distance from the joint marked with the same index.

As in every other manipulator system, the dynamic behavior, as a relationship between applied driving torques $\tau(u)$, environment forces h and joint motion trajectories $\ddot{q}, \dot{q}, q$, of mechanical joints can be described as [20]:

$$B(q)\ddot{q} + C(q,\dot{q})(\dot{q}) + G(q) + F_v\dot{q} + F_e q + F_d \mathrm{sgn}(\dot{q}) = \tau(u) - J^T(q)h \tag{1}$$

Here $q, \dot{q}$ and $\ddot{q}$ represent the three component joint angle, angular velocity and angular acceleration vectors. The *moments of inertia* are represented as a $(3 \times 3) B(q)$ matrix, while the second square matrix $C(q, \dot{q})$ expresses the *centrifugal* and *Coriolis* effects on the arm dynamics.

The *gravitational* contribution is expressed with a three element column vector, where every element g_i represents the moment generated at the joint i axis due to the presence of gravity:

$$G(q) = [g_1 \quad g_2 \quad g_3]^T, \tag{2}$$

where

$$g_1 = g_0 \left\{ [l_1 m_1 + a_1(m_2 + m_3)]\, c_1 + (l_2 m_2 + a_2 m_3) c_{12} + l_3 m_3 c_{123} \right\},$$
$$g_2 = g_0 \left[(l_2 m_2 + a_2 m_3 + a_2 m_3) c_{12} + l_3 m_3 c_{123} \right],$$
$$g_2 = g_0 l_3 m_3 c_{123}.$$

In this equation the cosines were simply denoted as $c_1 = \cos(q_1), c_{12} = \cos(q_1 + q_2)$ and $c_{123} = \cos(q_1 + q_2 + q_3)$. While the individual segment lengths a_i for a particular person were determined from IR markers used by a 3D positioning system, the masses m_i and gravity centers l_i, were obtained from the literature [15]. The gravitational acceleration g_0 was taken to be $9.81\ \mathrm{m/s^2}$.

The connection between the hand and the robot handle (see Section 3) creates a closed chain kinematic linkage. Thus, the end effector connection is described as a three dimensional vector with its horizontal and vertical forces (F_y, F_z) and the moment around the axis perpendicular to the plane of motion (M_x):

$$h = [F_y \quad F_z \quad M_x]^T \tag{3}$$

These forces have to be transformed to the joint level with the Jacobian matrix $J^T(q)$ as seen in the last product of Eq. 1. The joint muscle activity is expressed in terms of the active contribution $\tau(u)$, which is a function of muscle activation u.

The viscous contribution of the system is expressed in terms of $F_v\dot{q}$. $F_d \mathrm{sgn}(\dot{q})$ indicates the *dissipative* torques and is in the literature usually denoted as the static friction torque [20]. Finally, the *passive elastic torque* contributions in a particular joint are expressed with the product $F_e q$, where F_e is a diagonal matrix with the elements expressing the elasticity coefficients of every single joint.

Determining passive moments, as the sum of elastic and dissipative contributions, $F_e q + F_d \mathrm{sgn}(\dot{q})$ was the topic of this study. It has to be emphasized at this point, that $F_e(q)$ behaves non-linearly, where the diagonal elements are a function of all three joint angles. On the other hand, the term $F_d \mathrm{sgn}(\dot{q})$ contributes to the hysteresis observed later in Section 4.

3. The passive and static assumption

All measurement motions preprogrammed into the robot manipulator were slow, with arm joint angular speeds which did not exceed 0.3 rad/s for the elbow and 0.2 rad/s for the shoulder joint movement. The angular accelerations reached values of up to 1.2 rad/s^2 at points where the motion direction was altered, 0.6 rad/s^2 where the movement was started and ended and almost zero elsewhere. Because these were all verified to be very low values, the contributions of all dynamic terms in Eq. (1), were negligible compared to the non velocity and acceleration dependent terms:

$$B(q)\ddot{q} \approx 0, \quad C(q,\dot{q})\dot{q} \approx 0, \quad F_v\dot{q} \approx 0 \tag{4}$$

The next observation concerns the term $\tau(u)$ in Eq. (1). Because the subject was instructed before the experiment, to induce no voluntary muscle action whatsoever, a further assumption was made:

$$\tau(u) \approx 0 \tag{5}$$

To verify if this was justified, the EMG of a typical elbow flexion-extension trial was recorded prior to the large batch of experiments, to access the difference between active contribution of the person and inactivity. The surface electrodes were placed on the four major flexion and extension muscles by a skilled professional (i.e. biceps long and short head, triceps and brachioradialis). It is evident that no EMG activity in those muscles contributing to the movement was present (Fig. 2), confirming Eq. (5).

All these assumptions were accounted for in Eq. (1), modifying now to:

$$F_e q + F_s \mathrm{sgn}(\dot{q}) = -G(q) - J^T(q)h \tag{6}$$

The passive moments represented with the left side of Eq. (6) consist of the elastic contribution $F_e(q)$ and direction dependent dissipative moments $F_d\mathrm{sgn}(\dot{q})$ also known as Coulomb friction [20]. The passive moments can be summed up as a time and angle dependent column vector $\tau_p(q,t)$ or simply τ_p which was the focal point of this study:

$$\tau_p = [\tau_{p1} \quad \tau_{p2} \quad \tau_{p3}]^T \tag{7}$$

4. Measurement

In the performed experiment a positionally controlled antrophomorphic 6-DOF industrial robot (*Yaskawa© MOTOMANsk6*) was used for imposing a slow linear movement on the human arm in the sagittal plane (Fig. 3). A *JR*^{3}© 4 dimensional strain gauge force sensor was mounted on the manipulator end effector and used for force data collection. The maximum force for the specified output was $\pm$110 N, with an acquisition resolution of 12 bits. A bicycle-like circular rubber coated handle was mounted on top of the sensor in such a way, that rotation around the x axis was freely allowed. The next element in the system was a bus passenger seat, equipped with additional straps as evident from Fig. 3. The plane of motion was perpendicular to the ground and fully aligned with the sagittal plane of the subject. In the first part of the experiment, the subject was asked to keep his muscles relaxed while holding the handle.

The handle was held gently, while still allowing the arm to stay in good contact during the movement. Before starting the real measurements, it was also inspected whether the slight muscle activation due to

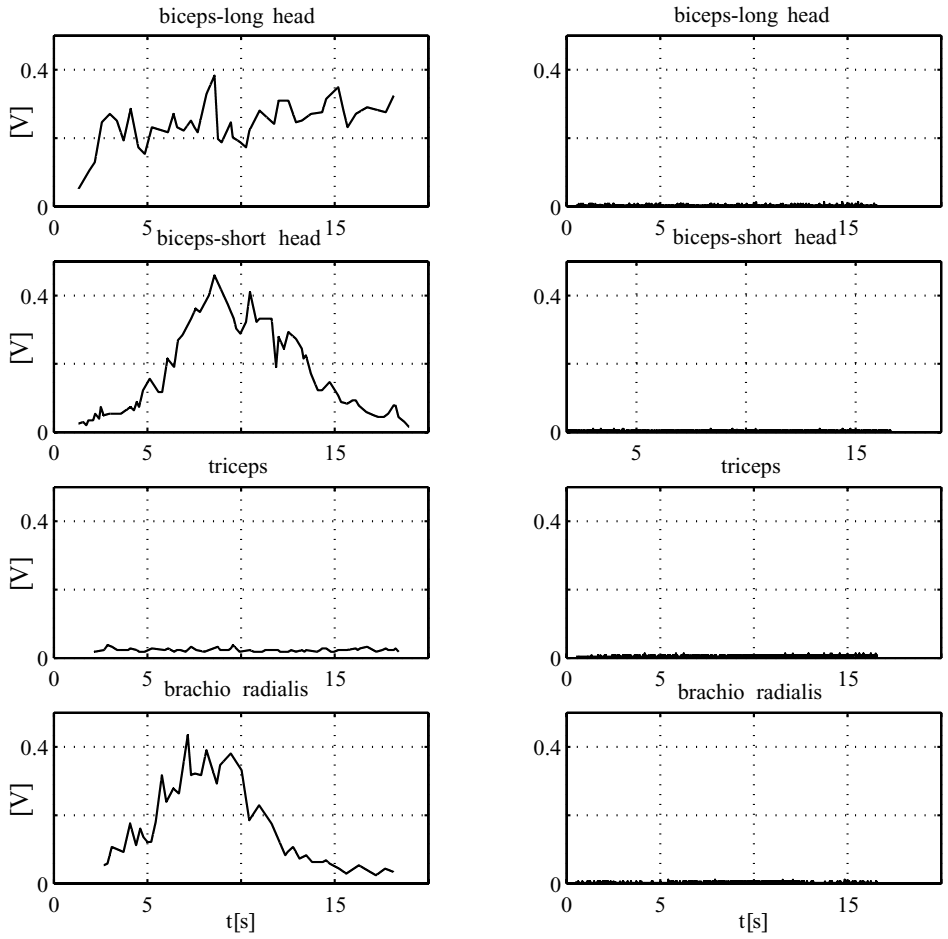

Fig. 2. EMG signals in the voluntary elbow flexion attempt (left column) and a passively held arm such as during the experiment (right column).

gripping had any significant effect on the passive torque identification process. No significant difference was found when comparing this data to the one when the hand was tightly strapped to the handle.

Due to the free handle rotation the hand dynamic parameters were properly adjusted. The mass and all geometric dimensions of the handle were accurately measured before the experiment. The handle mass m_{handle} was then added to the one of the hand m_{hand}, to yield a new third segment mass m_3, while the center of gravity locations l_{handle} and l_{hand} were also considered in obtaining a new location l_3:

$$\begin{aligned} m_3 &= m_{\mathrm{hand}} + m_{\mathrm{handle}}, \\ l_3 &= \frac{l_{\mathrm{hand}} m_{\mathrm{hand}} + l_{\mathrm{handle}} m_{\mathrm{handle}}}{m_{\mathrm{handle}} + m_{\mathrm{hand}}} \end{aligned} \tag{8}$$

Two main sets of measurements were made:

1. With the shoulder angle fixed at various angles, while the elbow angle was varied smoothly.
2. With the elbow fixed, while the shoulder was moved through a range of angles.

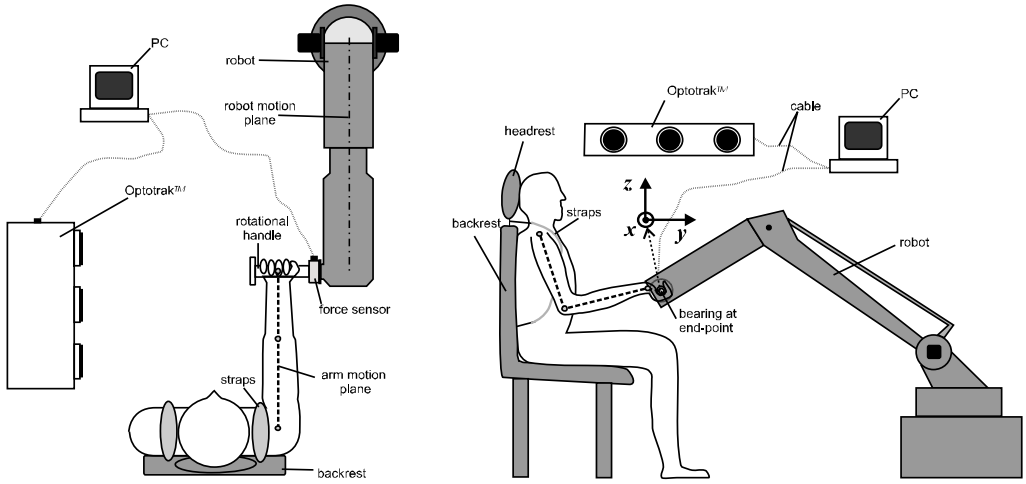

Fig. 3. Experimental setup from above (left) and a side view (right).

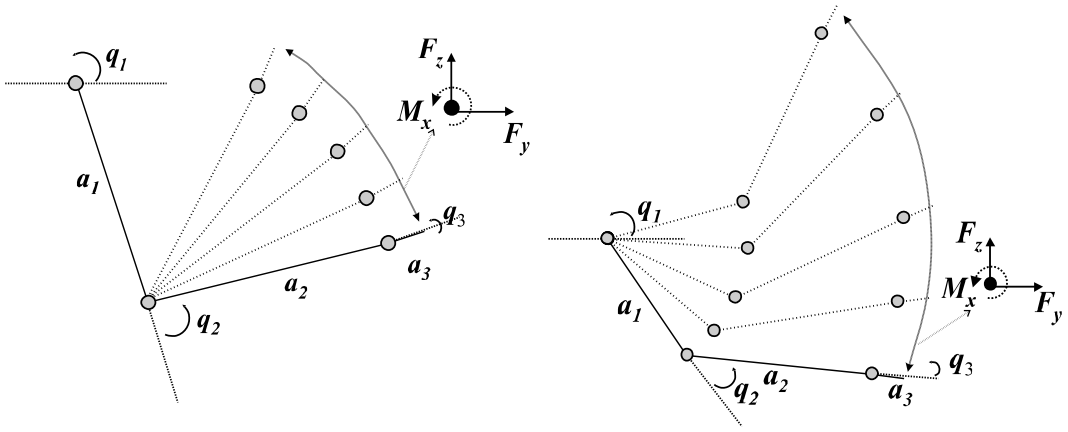

Fig. 4. A typical programmed elbow trajectory (left) at a certain fixed shoulder angle q_1 and shoulder trajectory (right) at a fixed elbow angle q_2.

In both cases the wrist was not fixed and was allowed to move freely since the deviation from the neutral position was found to be only a few degrees. Before the particular measurements, ten different circular trajectories (not shown here) were programmed into the robot for each subject. The first five measurements concentrated on the elbow angle smooth variation from one boundary angle to the other and backwards, with the shoulder fixed at different angles (-68°,-40°,$+16^\circ$,$+10^\circ$,$+36^\circ$). The shoulder angle was kept constant by programming an appropriate trajectory, using no additional fixation mechanisms Fig. 4–left side).

The second set of trials focused on movements of the shoulder joint, with the elbow kept at constant angles (20°, 30°,41°,49°,59°). For fixating the elbow angle, an orthosis was used, which allowed angle adjustments from extension to a flexion angle of 85 degrees (Fig. 4–right side).

The mass of the orthosis utilized for shoulder movements was included into the calculation of the $G(q)$ matrix in Eq. (2), which describes the new upper and forearm masses and center of gravity locations as

m_i and l_i:

$$\begin{aligned} m_1 &= m_{ua} + m_{uo}, \;\; m_2 = m_{fa} + m_{lo} \\ l_1 &= a_1 - \frac{l_{ua}m_{ua} + l_{uo}m_{uo}}{m_{ua} + m_{uo}} \\ l_2 &= \frac{l_{fa}m_{fa} + l_{fo}m_{fo}}{m_{fa} + m_{fo}} \end{aligned} \tag{9}$$

Here the ua and fa indices refer to the *upper* arm and *forearm*, whereas uo and fo describe the *upper* and *lowerorthosis* parts. The orthosis masses and centers of gravity were accurately determined before the experiment.

A 3D tracking system *Optotrak*© was used to precisely record the movements during the experiment. The IR markers were attached to the skin above the rotation points of the three arm joints in consideration, to the handle and to robot manipulator joints to allow for later verification and complete reconstruction of the measurement. All calculations mentioned here were performed off-line using Matlab© The Optotrak© and Force sensor data were both lowpass filtered at 5 Hz using a sixth order Butterworth filter provided by the Matlab© Signal Processing toolbox.

Six healthy subjects were tested with body masses ranging from 64 kg to 77 kg. They were all right-handed males aged from 25 to 39 years. None had ever suffered from any kind of neuromuscular disease. All were asked to sit in a chair, lightly grip the robot attached handle and not exert any voluntary muscle action. Before the experiment at least two preliminary movements were made to assure that the programmed trajectory was appropriate and that the subject was comfortable. After defining 10 different trajectories a set of the first ten movements was measured for the elbow and the second ten, for the shoulder joint.

Initially, six twenty-trial sets were made on one particular subject (age 25, weigh 77 kg), with every set performed on a separate day. Every movement was repeated six times, for a total of sixty measurements. Hence, all together six measurements were made for the every movement (i.e. extension to flexion and backwards). All other subjects were only measured twice for every movement.

5. Results

The results section is composed of two parts. First, a detailed overview of data acquired for one intact person is given. Among checking the general trends the purpose of this batch was to assess fidelity and repeatability of the method. The second part includes measurements on six persons to gain insight into data variability among several persons.

It has to be noted that for these measurements the shoulder and elbow were not moved throughout their complete range of motion because of a limitation imposed by the working space of the robot manipulator. Due to that, the exponential nature of the passive moments for intact population, which is more expressed near the articular boundaries, is in these results not always evident. Because of this fact the passive moment values are sometimes of very low value and therefore realistically also a subject to larger errors.

5.1. Passive moment results for one subject

Initially, six measurements of all ten movements were made on one particular subject (age 25, weight 77 kg), with every one performed on a separate day.

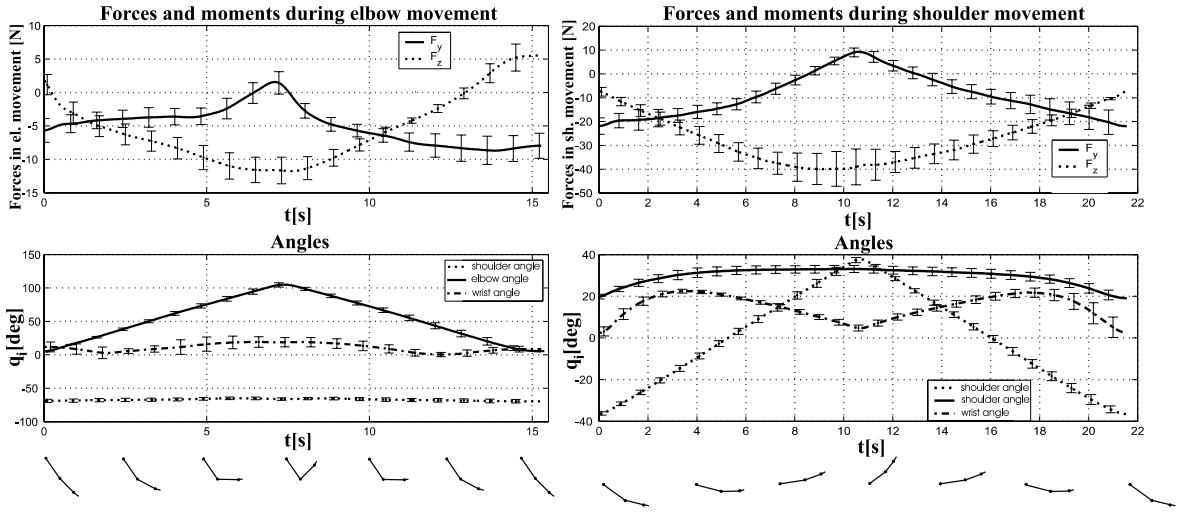

Fig. 5. The average handle force h and joint angle q_i trajectories with their standard deviation error bars in six trials, in an elbow movement while the shoulder was fixed at $q_1 \approx -68^\circ$ (left column) and in a shoulder movement while the elbow was fixed at $q_2 \approx 27^\circ$ (right column). The arm movement is sketched below the figure.

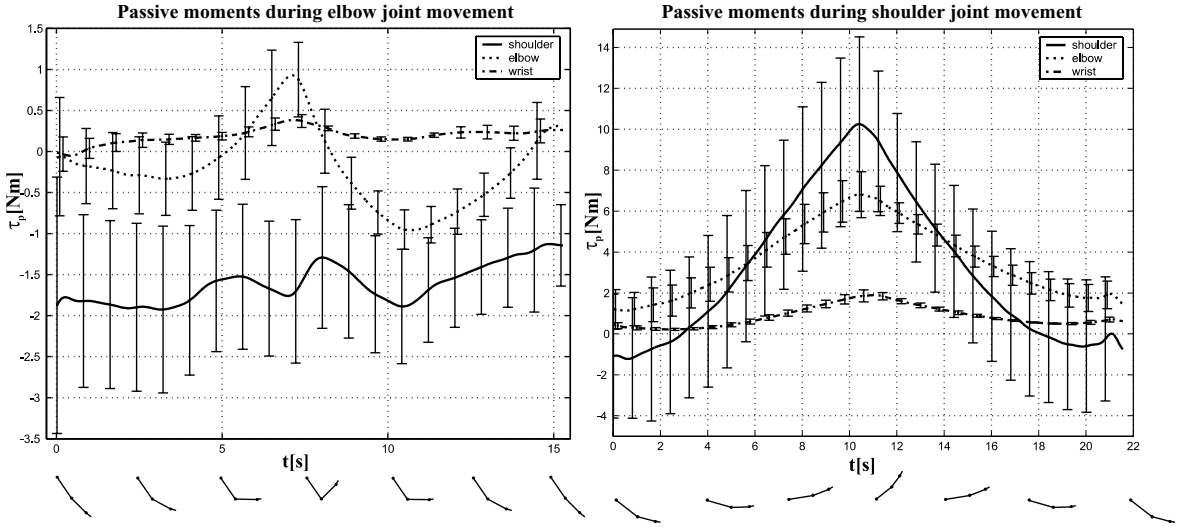

Fig. 6. The average passive moments in all three joints, computed from the data in Fig. 5 (above) with their standard deviation error bars, in an elbow movement while the shoulder was fixed at $q_1 \approx -68^\circ$ (left column) and in a shoulder movement while the elbow was fixed at $q_2 \approx 27^\circ$(right column). The arm movement is sketched below the figure.

In total six measurements were made for every movement (i.e. extension to flexion and backwards). In Fig. 5 average time courses and six-trial standard deviations of force and kinematic data for one fixed-elbow and one fixed-shoulder configuration, are shown (the other eight configurations are not shown here due to lack of space). Note that the scale in the right column of Fig. 5 is much larger than the one in the left. The force data deviations are also larger in both plots than the ones of kinematic data.

The x axis torque M_x was negligible due to a bearing attached in the mechanism of the handle and is not shown. These averaged data were then applied to the Eq. (6), yielding a vector of average passive

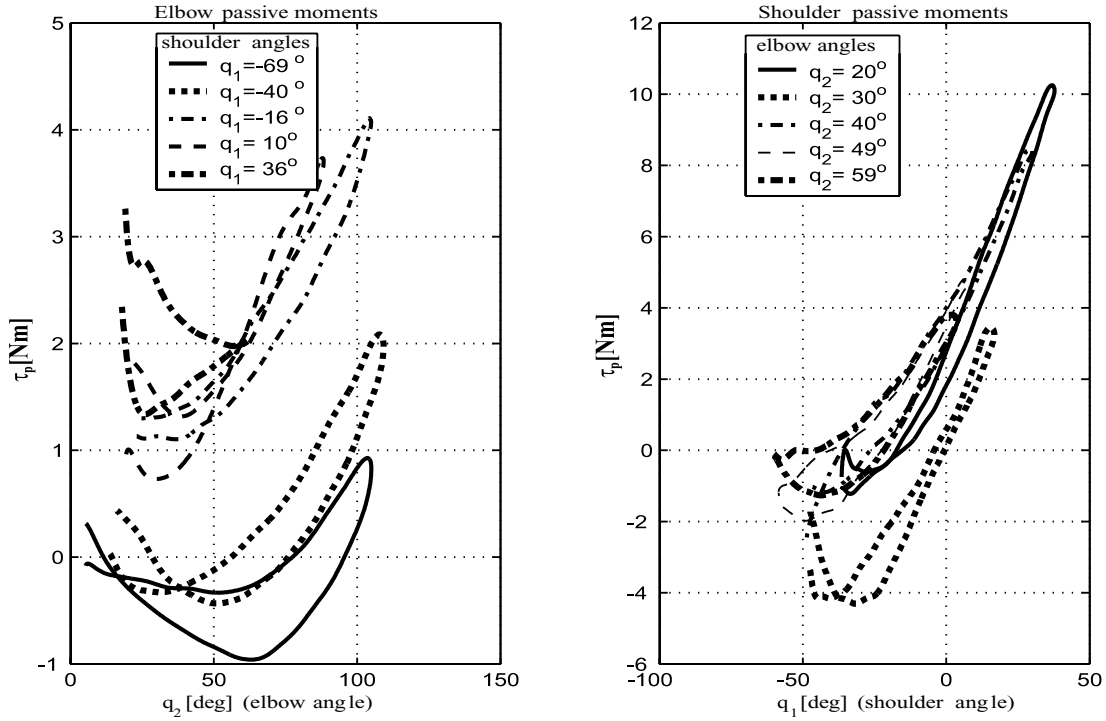

Fig. 7. All five average elbow (left) and shoulder (right) passive moments as a function of both angles for the same person. Every curve represents an average of six measurements.

Table 1
Maximum elbow passive moment standard deviations from average (as seen in the left side of Fig. 7) at five different shoulder fixation angles

	$\sigma_{\max}(q_1 = -69^\circ)$	$\sigma_{\max}(q_1 = -40^\circ)$	$\sigma_{\max}(q_1 = -16^\circ)$	$\sigma_{\max}(q_1 = 10^\circ)$	$\sigma_{\max}(q_1 = 35^\circ)$
elbow passive moment (τ_{p2})	0.7 Nm	1.1 Nm	1.0 Nm	0.4 Nm	1.1 Nm

Table 2
Maximum shoulder passive moment standard deviations from average (as seen in the right side of Fig. 7) at five different shoulder fixation angles

	$\sigma_{\max}(q_2 = 20^\circ)$	$\sigma_{\max}(q_2 = 30^\circ)$	$\sigma_{\max}(q_2 = 40^\circ)$	$\sigma_{\max}(q_2 = 49^\circ)$	$\sigma_{\max}(q_2 = 59^\circ)$
shoulder passive moment (τ_{p1})	4.4 Nm	3.6 Nm	2.7 Nm	3.0 Nm	2.2 Nm

moments $\overline{\tau}_p$ for these two configurations (Fig. 6). Again the scale in the right side of Fig. 6 is much larger.

It is sensible to represent the passive moments in relation to the displaced angle, which can be seen in Fig. 7. The fixation angles of the elbow (q_2) and shoulder (q_1) as measured by the Optotrak system, are also denoted.

Clearly the passive moments of the shoulder are much less influenced by adjacent angle fixation than the ones of the elbow. This comes as a result of a smaller number of passive muscles spanning the elbow joint (7) compared to a much greater number of muscles in the shoulder (15). The maximum standard deviations $(\sigma_{\max})$ acquired for every passive moment seen in Fig. 7 can be seen in Tables 1 and 2.

It is obvious that these standard deviations are quite large, contributing to a large relative error at

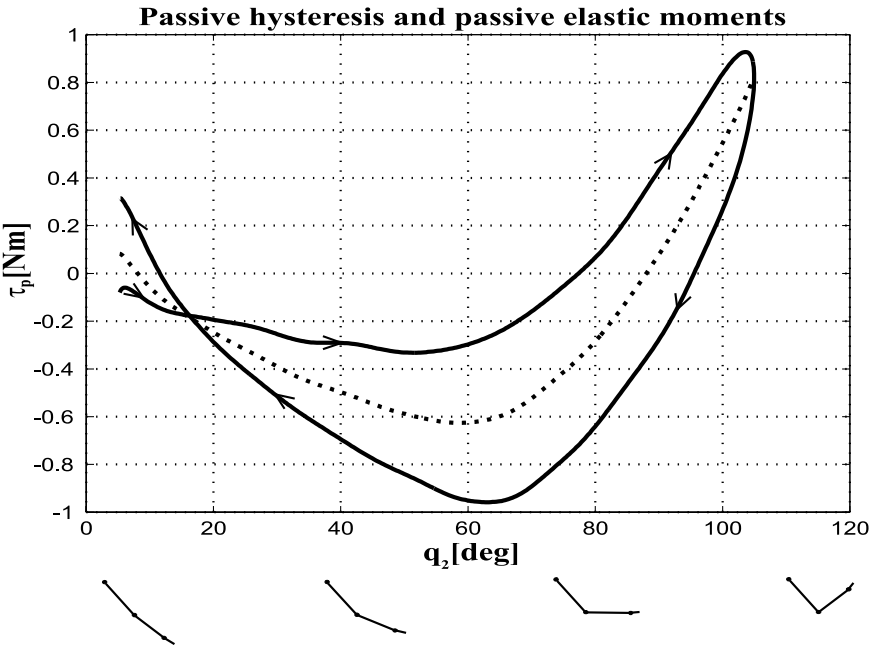

Fig. 8. Elbow passive moment hysteresis (solid line) with the elastic moment (dashed line) and the movement direction (arrow). Below the figure the arm movement scheme is depicted. The shoulder angle was fixed at $q_1 \approx -68^\circ$.

points where passive moment values are around zero. This error is mostly due to a large force standard deviation, which was observed in Fig. 5.

It has to be noted that in Fig. 7, the range of displaced angles was different for every particular movement because of different joint movement ranges at corresponding adjacent angle fixations. In all curves a hysteresis arising due to muscle dissipative effects can clearly be observed [12], where the upper part of the curve always indicates movements from extension to flexion. The hysteresis average is known to be the passive elastic moment, which was the interest of some earlier studies [13,19] and can also be seen from Fig. 8 for a typical elbow trajectory (at shoulder fixation). The passive moment curve patterns show an ascending pattern most of the time, at small angles, however, this is sometimes a descending one resulting in a global minimum.

5.2. Passive moment results for six subjects

The same data analysis was used for all six subjects in the study and all measurements were made under the same conditions. Every movement was measured twice for every subject.

It needs to be emphasized that for practical reasons the shoulder and elbow angles were not fixed completely equally for all subjects. This is mostly due to a fairly complex process of trajectory programming and different arm geometry among subjects. This fact inseparably results also in slightly different passive moments. Similar standard deviations as with one subject were observed. To limit the presentation space here, only two of the ten calculated passive moments for all subjects are shown. To show the variation of results among all six subjects, only traces for two different movements are shown in Fig. 9. It should again be noted that the scale of shoulder passive moments is larger than for elbow passive moments.

Every curve in this plot represents an average of two measurements. Most subjects show a similar pattern, although some show quite obvious differences in the hysteresis size and slope. However, it can

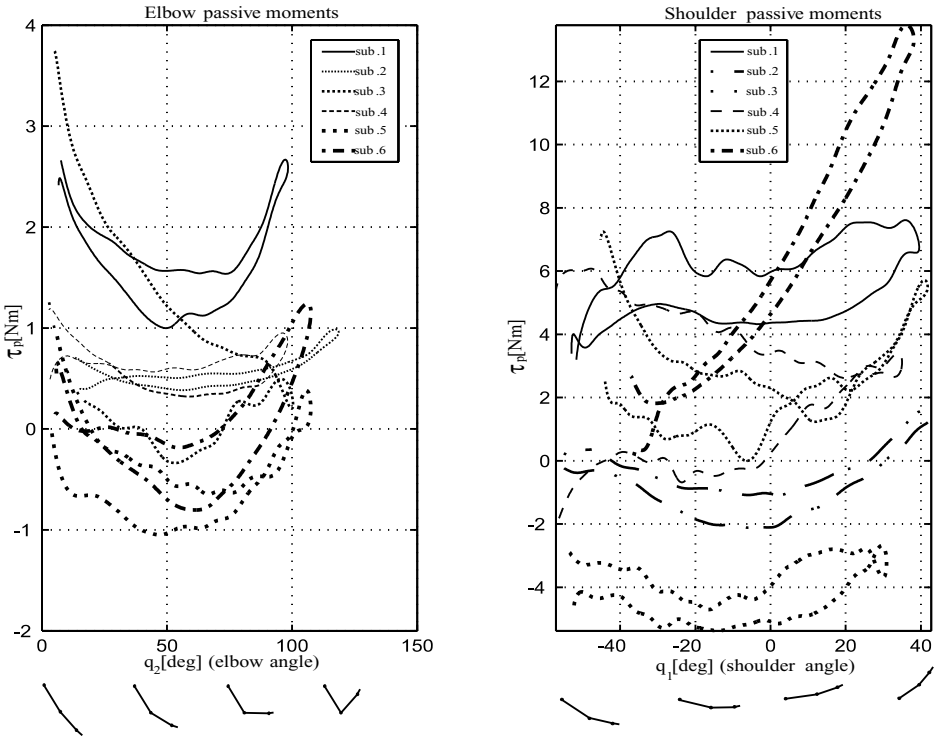

Fig. 9. Obtained passive moments for all six subjects performing two particular movements when the shoulder joint was fixed at $q_1 \approx -63^\circ$ (left) and the elbow joint at $q_2 \approx 27^\circ$ (right). Every point was obtained as an average of two measurements.

be concluded that most curves show a similar pattern.

6. Discussion and conclusion

In this paper a method for estimating arm passive moments is proposed, which according to our knowledge has not been used before. Similar angle-dependent studies have been made before for the lower extremities [19,25], while the upper extremity passive moments were not studied as much. In the measurement process, firstly one healthy individual was studied more in detail as described in Section 3. The repeatability of data obtained from six measurements can be observed in Fig. 5. While the angle data is very repeatable, the force sensor data on the other hand, shows more deviations. This is caused by a difficulty with which a subject is capable of maintaining the arm-robot connection fully equally in two successive trials. These raw data were then applied to Eq. (6), producing a passive moment vector, represented in Fig. 6 as a function of time. From this vector τ_{p2} represents the elbow passive moment and τ_{p1} the shoulder passive moment. Five elbow and five shoulder passive moments were inspected, with adjacent joints being fixed at various angles (Fig. 7). In addressing the repeatability issue, it can be observed that every curve obtained on a separate day, shows a similar pattern. The amplitude variations arise mostly from the errors in the measurement process.

Furthermore, five more healthy subjects were measured in the same way. The force and kinematic data among subjects show larger deviations than for one subject, due to geometrical and dynamical differences (not shown in this paper). This also explains why there is no straightforward correlation in

the passive moments among all subjects (Fig. 9). Just two passive moments are being presented, while the other eight are not shown in order to limit the presentation space. A large amplitude variation among different subjects was observed, especially in the shoulder joint.

It can be seen that the passive moments are strongly influenced by adjacent joint fixation. However, this is much less evident for the shoulder joint, as it is for the elbow (Fig. 7). It is also obvious that the shoulder passive moments are far larger than the ones obtained for the elbow. The reason lies in passive one and two-joint muscles, which span over both joints and are very likely the major contributor to the passive properties. While there are only seven muscles producing elbow joint movements, there are fifteen, which are involved in the shoulder, with a total cross section area far greater than the one of the elbow muscles. Apart from this, the biceps and triceps muscles, which contribute to elbow joint motions are two-joint muscles spanning the whole upper arm and hence influence the passive properties of both the shoulder and the elbow joint.

In all similar works the passive elastic torque was found to resemble a symmetrical double exponential curve with highly positive values at complete extension and negative ones at extreme flexion. Other parts of the curve were found to be almost linear. It needs to be emphasized that the passive moments in this study, contain elastic and dissipative contributions as explained in Eq. (6) and seen in Fig. 8. The calculated average passive moment patterns observed in Figs 7 and 9, sometimes show a descending tendency at low angles. The reasons for this lies in the fact that the gravity contributions $G(q)$ from Eq. (6) have a larger inverse tendency than the environment contributions $J^T(q)h$ in that particular angular region. With the continuing flexion motion, however, the passive moments always show an increasing trend.

It has to be underlined that the flexion-extension movement limits in this study never reached the articular boundaries of either the elbow or the shoulder joint. This occurs due to a limited robot workspace and almost no physical constraining of the arm. Therefore the passive moments were quantified only in the central region of the movement range. The calculated passive moments here are also opposite in sign and show an inverse tendency compared to many other studies because the angle notation is different.

Apart from the relatively large force sensor data deviations (Fig. 5), another source of error is also the term $G(q)$ in Eq. 6 which was calculated by using the segment masses m_i, lengths a_i and centers of gravity l_i, from the literature [15]. Because the segment mass estimation m_i affects only the term $G(q)$ in this equation, the inexact value causes significant errors to the passive moment calculation. A comprehensive analysis on these errors would be very beneficial in the future. On the other hand, segment length and center of gravity location errors do not affect the result greatly. The effect they have on the term $G(q)$ cancels itself with that from the environment contribution term $J^T(q)h$ (Eq. 6). The reason lies in the Jacobian matrix $J^T(q)$ which also depends on l_i and a_i. Hence, the error imposed by a marker misalignment, is not very prominent, resulting in low percentage changes in segment lengths a_i and subsequently centers of gravity l_i.

Owing to the fact that the planar model structure is mathematically far less complex to describe than any other alternative, some studies suggest that the motor control system in the human brain actually uses a simplified version of such a model in determining the inverse dynamics problem [21]. In the model used in this study, the segments are presumed to be rigid, while the joints include pure rotation without any translation. Apart from that, the shoulder complex also includes two translational degrees of freedom. The study of Veeger et al. [22] shows that the flexion-extension rotational center translation of the glenohumeral joint was within just 4 mm of the geometric center, making our assumption reasonably justified.

The study presented here simultaneously determines all three passive moments from the inverse dynamics model by using a robot manipulator. If compared to other studies on passive moments, the

method seems to be elegant from the subject point of view, with less physical constraining of particular arm segments required. The single required constraining mechanism in the process is the elbow orthosis, utilized for all shoulder movement trajectories, whereas all elbow motion trajectories are performed with all arm joints being completely unconstrained. Moreover the methods used for assessing the passive moments in other studies concentrate on masses and other dynamic parameters of the body segment in motion, enabling the determination of passive moments for only one considered joint.

The experimental results shown here were obtained for healthy individuals with an experimental setup using an industrial robot as the main apparatus. We expect that impaired subjects that we would like to measure in the future should show values clearly distinguishable from the results on intact subjects. Such measurements would be useful on patients with neuromuscular disorders, usually following a stroke or some neuromuscular disease. These patients are considered to be good candidates for treatment with new rehabilitation treatment devices such as haptic robots, which allow human machine interaction by means of force and touch. In these environments the methodology shown here would represent a measurement module. Such a method has the power to provide an alternative upper extremity clinical evaluation method, which could provide results instantaneously during the rehabilitation practice itself.

Acknowledgements

The authors would like to thank Prof. Garth R. Johnson from the University of Newcastle for his assistance during the initiation of this work and comments to the manuscript. This work was stimulated by the European Community project GENTLE/S–Quality of life under Framework 5.

Nomenclature

$B(q)$ =moment of inertia matrix
$C(q, \dot{q})$ =Coriolis matrix
$G(q)$ =gravity matrix
F_y =horizontal force component
F_z =vertical force component
F_d =dissipative coefficient matrix
F_e =elastic coefficient matrix
F_v =viscous coefficient matrix
I_i =arm segment inertia
J^T =Jacobian matrix transpose
M_x =torque around x axis (perpendicular to the motion plane)
a_i =segment length
h =vector of end effector forces and moments
l_i =segment center of gravity location
l_{hand} =hand center of gravity location
l_{handle} =rotating handle center of gravity location
m_i =segment mass
m_{fa} =forearm mass
m_{lo} =lower orthosis part mass
m_{ua} =upper arm mass

m_{uo} =upper orthosis part mass
m_{hand} =hand mass
m_{handle} =mass of rotating handle
q =joint angle vector
$\dot{q}$ =joint velocity vector
$\ddot{q}$ =joint acceleration vector
τ_p =passive moment vector
$\tau(u)$ =voluntary muscle torque

References

[1] A.M. Acosta, R.F. Kirsch and E.J. Perreault, A robotic manipulator for the characterization of two-dimensional dynamic stiffness using stochastic displacement perturbations, *Journal of Neuroscience Methods* **102** (2000), 177–186.
[2] M.L. Audu and D.T. Davy, The influence of muscle model complexity in musculoskeletal motion modeling, *Journal of Biomechanical Engineering* **107** (1985), 147–156.
[3] D.J. Bennett, Torques generated at the human elbow joint in response to constant position errors imposed during voluntary movements, *Experimental Brain Research* **95** (1993), 488–498.
[4] D.J. Bennett, J.M. Hollerbach, Y. Xu and I.W. Hunter, Time varying stiffness of human elbow joint during cyclic voluntary movement, *Experimental Brain Research* **88** (1992), 433–442.
[5] A.E. Engin and S.M. Chen, Statistical Data Base for the biomechanical properties of the human shoulder complex I: Kinematics of the shoulder complex, *Journal of Biomechanical Engineering* **108** (1986), 215–221.
[6] A.E. Engin and S.T. Tumer, Three-dimensional kinematic modelling of the human shoulder complex–Part I:Physical model and determination of joint sinus cones, *Journal of Biomechanical Engineering* **111** (1988), 107–112.
[7] A.E. Engin and S.T. Tumer, Three-dimensional kinematic modelling of the human shoulder complex–Part II: Mathematical modeling and solution via optimization, *Journal of Biomechanical Engineering* **111** (1988), 113–121.
[8] A.E. Engin and S.M. Chen, Statistical Data Base for the biomechanical properties of the human shoulder complex–II: Passive resistive properties beyond the shoulder complex sinus, *Journal of Biomechanical Engineering* **108** (1986), 222–227.
[9] A.E. Engin and S.M. Chen, Kinematic and passive resistive properties of human elbow complexon, *Journal of Biomechanical Engineering* **109** (1987), 318–323.
[10] A.E. Engin, R.D. Peindl, N. Berme and I. Kaleps, Kinematic and force data collection in biomechanics by means of sonic emitters– I: Kinematic data collection methodology, *Journal of Biomechanical Engineering* **106** (1984), 204–211.
[11] A.E. Engin, R.D. Peindl, N. Berme and I. Kaleps, Kinematic and force data collection in biomechanics by means of sonic emitters– II: Force data collection and application to the human shoulder complex, *Journal of Biomechanical Engineering* **106** (1984), 212–219.
[12] A. Esteki and J.M. Mansour, An experimantally based nonlinear viscoelastic model of joint passive moment, *Journal of Biomechanics* **29** (1996), 443–450.
[13] H. Hatze, A three-dimensional multivariate model of passive human joint torques and articular boundaries, *Clinical Biomechanics* **12** (1997), 128–135.
[14] F.C.T. Van der Helm, Analysis of the kinematic and dynamic behavior of the shoulder mechanism, *Journal of Biomechanics* **27** (1994), 527–550.
[15] P. de Leva, Adjustments to Zatsiorsky-Seluyanov's segment inertia parameters, *Journal of Biomechanics* **29** (1995), 1223–1230.
[16] J.M. Mansour and M.l.L. Audu, The passive elastic moment at the knee and its influence on human gait, *Journal of Biomechanics* **5** (1996), 369–373.
[17] E.J. Perreault, P.E. Crago and R.F. Kirsch, Estimation of intrinsic and reflex contributions to muscle dynamics: A modelling study, *IEEE transactions on biomedical engineering* **47** (2000), 1413–1421.
[18] E.J. Perreault, R.F. Kirsch and P.E. Crago, Effects of shoulder stability on endpoint stiffness, *IEEE engineering in medicine and biology* (November/December 2000), 53–58.
[19] R. Riener and T. Edrich, Identification of passive elastic moments in the lower extremities, *Journal of Biomechanics* **32** (1999), 539–544.
[20] L. Siciliano and B. Sciavicco, *Modeling and control of robot manipulators*, The McGraw-Hill Companies, Inc, 1996.
[21] M. Suzuki, Y. Yamazaki and K. Matsunami, Simplified dynamics of planar two-joint arm movements, *Journal of biomechanics* **33** (2000), 925–931.

[22] H.E.J. Veeger, B. Yu, K. An and R.H. Rozendal, Parameters for modeling the upper extremity, *Journal of Biomechanics* **30** (2000), 647–652.
[23] Y. Xu and J.M. Hollerbach, A robust ensemble data method for identification of human joint mechanical properties during movement, *IEEE transactions on biomedical engineering* **46** (2000), 409–419.
[24] Y. Xu and J.M. Hollerbach, Identification of human joint mechanical properties from single trial data, *IEEE transactions on biomedical engineering* **45** (1998), 1051–1059.
[25] Y.S. Yoon and M. Mansour, The passive elastic moments at the hip, *Journal of Biomechanics* **12** (1982), 905–910.